**Ocean Systems Engineering**, *Vol. 8, No. 3 (2018) 313-327*
DOI: https:// doi.org/10.12989/ose.2018.8.3.313 

# Investigation of touchdown point mismatch during installation for catenary risers

Chaojun Huang[a], Guanyu Hu[b] and Fengjie Yin*

*2H Offshore Inc., 15990 N Barkers Landing Rd, Houston, TX 77079, USA*

*(Received July 17, 2018, Revised August 9, 2018, Accepted August 12, 2018)*

**Abstract.** Meeting the touchdown point (TDP) target box is one of the challenges during catenary riser installation, especially for deep water or ultra-deep water riser systems. TDP location mismatch compared to the design can result in variation of riser configuration, additional hang-off misalignment, and extra bending loads going into the hang-off porch. A good understanding of the key installation parameters can help to minimize this mismatch, and ensure that the riser global response meets the design criteria. This paper focuses on investigating the potential factors that may affect the touchdown point location, and addressing the challenges both in the design stage and during installation campaign. Conventionally, the vessel offset and current are the most critical factors which may affect the TDP movement during installation. With the offshore exploration going deeper and deeper in the sea (up to 10,000ft), other sources such as the seabed slope and seabed soil stiffness are playing an important role as well. The impacts of potential sources are quantified through case studies for steel catenary riser (SCR) and lazy wave steel catenary riser (LWSCR) in deep water application. Investigations through both theoretical study and numerical validation are carried out. Furthermore, design recommendations are provided during execution phase for the TDP mismatch condition to ensure the integrity of the riser system.

**Keywords:** TDP; target box; SCR; LWSCR; misalignment; mismatch; installation; deep water; integrity

## 1. Introduction

Risers are among the most important components of offshore oil and gas platforms. Risers are the conduits between the subsea wellhead and the drilling or production platform for development, production, gas lift or water injection purposes. Catenary riser configuration is the most popular riser configuration for deepwater oil production beyond 1000 meter water depth, either in pure catenary shape or lazy wave catenary shape.

All global analyses for subsea risers in catenary shape are normally conducted for the designed configuration (Yue *et al.* 2010, 2011, Santala *et al*. 2017). A target box of the touchdown point (TDP) is typically specified for the subsea installation contractor to meet the tolerance of design configuration during installation. Installation of catenary riser can be quite challenging and costly (Antony *et al*. 2017). Hoffman *et al.* (2010) studied the many challenges in design and installation

∗Corresponding author, Ph.D., E-mail: Fengjie.Yin@2hoffshore.com
[a] Ph.D., E-mail: Chaojun.Huang@2hoffshore.com
[b] Ph.D., E-mail: Guanyu.Hu@2hoffshore.com


http://www.techno-press.org/?journal=ose&subpage=7 ISSN: 2093-6702 (Print), 2093-677X (Online)

of the “worlds first” lazy wave SCR system. Thomas *et al.* (2010) also studied the challenges during the installation of a steel lazy wave riser. However, it is one of the biggest challenges to meet the TDP target box during catenary riser installation, especially for deep water or ultra-deep water riser systems. Various factors can impact the riser configuration during riser installation stage. It is very possible to miss the TDP target box during a severe environmental event, such as loop currents.

Missing the TDP target box may result in unexpected system failure without further evaluation of the new riser configuration. It is very important to find the source causing the TDP mismatch and root out the permanent TDP mismatch, which may cause system failure. This paper focuses on evaluating the potential sources for TDP mismatch through both theoretical study using catenary equations and numerical validation using finite element software.

## 2. Catenary equation and typical catenary riser configurations

Though deepwater risers are usually made of steel and have very large bending stiffness, their bending stiffness can be ignored when calculating the static configuration due to their large aspect ratios. The static configuration of a steel catenary (SCR) riser can be simplified as the catenary function shown in Fig.1 and Eq. (1).

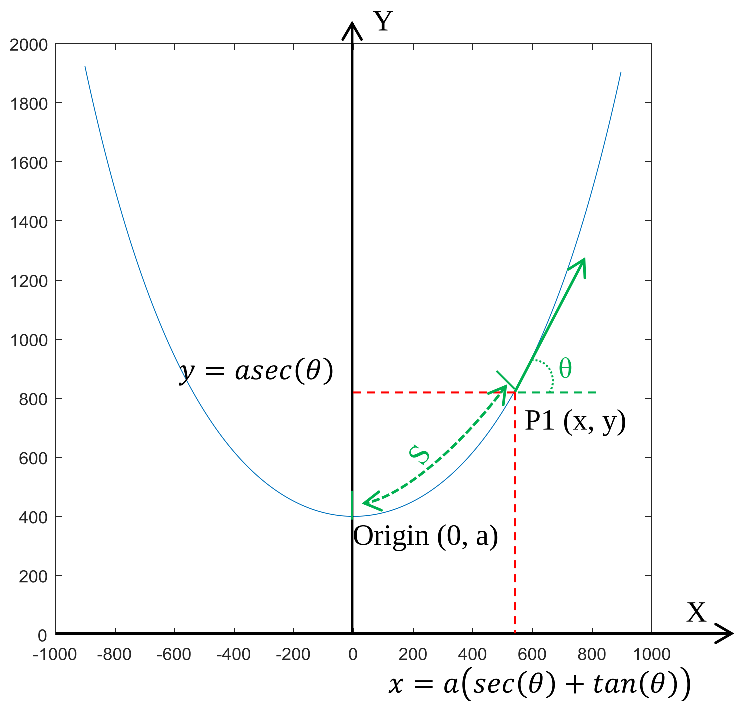


Fig. 1 Catenary equations

$$S = a \tan\theta$$
$$x = a \ln(\sec\theta + \tan\theta) \quad (1)$$
$$y = a \sec\theta$$

Where:

- $S$ is the arc length from the origin $(0,\ a)$ to P1 $(x,\ y)$.
- $\theta$ is defined as the tangential slope angle at a point (P1).
- $a$ is defined as the catenary shape parameter.

### *2.1 Catenary riser configuration*

For a typical SCR configuration shown in Fig. 2, the hang-off angle (top departure angle) of (90°- $\theta_1$) and the height ($Y$) between hang-off point and seabed are usually known. The TDP to hang-off distance $X$ is defined as the $(X_1 - X_2)$. Taking all the known parameters into equation 1, the suspended length ($S$) and TDP to hang-Off horizontal distance ($X$) of SCR can be calculated by solving the following equations (Singh and Bhatt 2010) assuming rigid seabed.

$$X = X_1 - X_2 = a\big(ln(\sec\theta_1 + \tan\theta_1) - ln(\sec\theta_2 + \tan\theta_2)\big) \quad (2)$$
$$Y = Y_1 - Y_2 = a(\sec\theta_1 - \sec\theta_2)$$

where $\theta_2$ is the seabed slope, can be positive and negative. It is 0 for flat seabed. Friction is ignored in a sloped seabed condition.

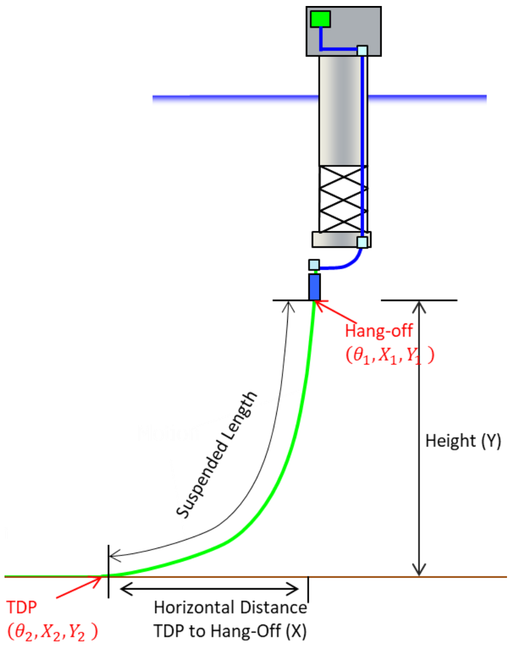


Fig. 2 Typical catenary riser configurations

### *2.2 Lazy wave catenary riser configuration*

The static behavior of a lazy wave riser was briefly studied by Li and Nyuen (2010), Wang *et al.* (2013), and Queau *et al.* (2013). Li and Nyuen (2010) thoroughly introduced the catenary equation and the static configuration of a lazy wave riser with flat seabed using Cartesian system. Wang *et al.* (2013) proposed similar static configuration equations with flat seabed for LWSCR and numerically implemented using MATLAB, while Queau *et al.* (2013) expanded the static equations by including the flat seabed soil stiffness. In this paper, a much more simplified LWSCR static configuration model (see Eq. (3)) is proposed using Whewell equations in Cartesian system while also considering the seabed slope.

For a typical lazy wave SCR (LWSCR) configuration shown in Fig. 3, the static configuration can be separated into three catenary sections:

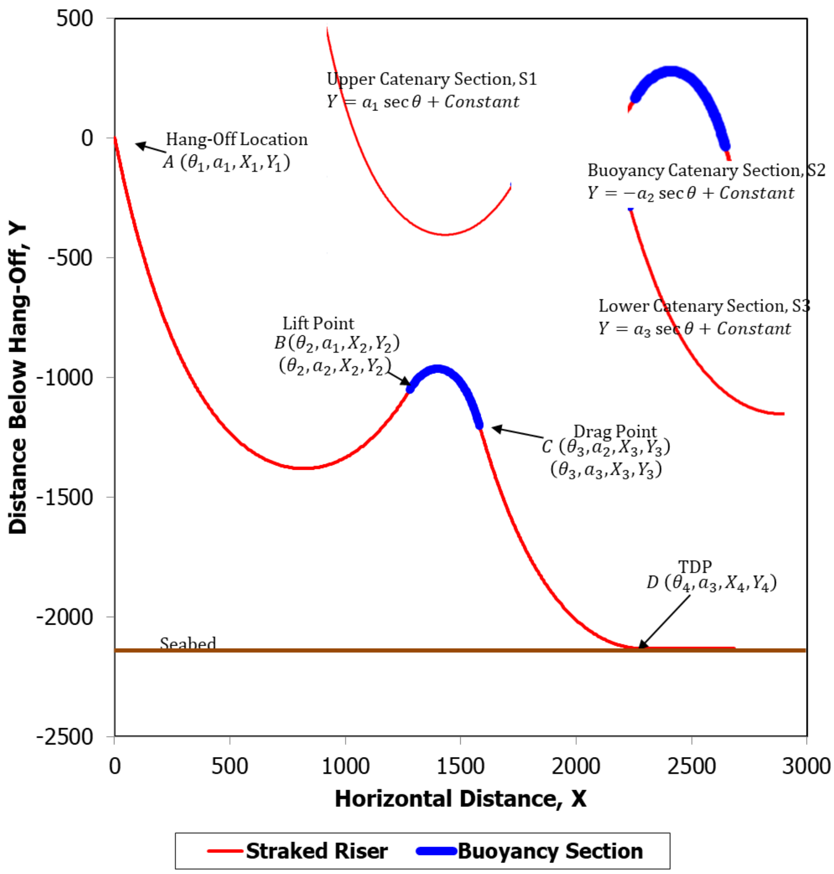


Fig. 3 Typical LWSCR configurations

- **Upper catenary section ($S1$)**: defined from hang-off to start of the buoyancy section. It is a regular catenary function with a shifting of origin.
- **Buoyancy catenary section ($S2$)**: defined from the start of buoyancy section to the end of buoyancy section. It is an upside-down catenary function (due to uplift force direction) with a shift of origin.
- **Lower catenary section ($S3$)**: defined from end of buoyancy section to TDP. It is the same as a regular SCR.

Using three catenary functions, known parameters (such as hang-off angle, wet unit weight for each section, hang-off height and lengths of the first two sections), balance of force at lift point and drag point, the static configuration of a LWSCR can be calculated using the following set of equations

$$\begin{cases} S_1 = a_1(\tan\theta_2 - \tan\theta_1) \\ S_2 = a_2(\tan\theta_2 - \tan\theta_3) \\ S_3 = a_3(\tan\theta_3 - tan\,\theta_4) \\ a_1 \tan\theta_2\, m_1 g + a_2 \tan\theta_2\, m_2 g = 0 \\ a_3\,(\tan\theta_3 - tan\,\theta_4)\, m_3 g + a_2 \tan\theta_3\, m_2 g = 0 \\ Y = a_1(\sec\theta_2 - \sec\theta_1) + a_2(\sec\theta_2 - \sec\theta_3) + a_3(\sec\theta_3 - \sec\theta_4) \\ X = a_1(\mathrm{x}(\theta_2) - \mathrm{x}(\theta_1)) + a_2(\mathrm{x}(\theta_3) - \mathrm{x}(\theta_2)) + a_3(\mathrm{x}(\theta_3) - \sec\theta_4) \end{cases} \quad (3)$$

where,

- $\theta_1, \theta_2, \theta_3$ and $\theta_4$ are the tangential angle at hang-off location, lift point, drag point and TDP, respectively.
- $S_1, S_2, S_3$ are the arc lengths for upper, buoyancy and lower catenary section with $a_1, a_2$ and $a_3$ as corresponding catenary shape parameters, $m_1, m_2$ and $m_3$ as corresponding wet unit weight, g as the gravitational acceleration. Usually $m_1 = m_3$ and $\theta_4 = 0$, hence, $a_1$=$a_3$.
- $\mathrm{x}(\theta)$ represents $\ln(\sec\theta + \tan\theta)$ +*constant*.

## 3. Critical factors for TDP locations

Based on the equations for SCR and LWSCR, other than installation errors, the critical factors which can impact the TDP locations include vessel offset, bottom current during installation, seabed properties, riser wet weight and buoyancy uplift.

### *3.1 Vessel offset*

Vessel position has a large impact on the configuration of riser, thus on the TDP locations. Vessel offset is usually controlled to be small during riser installation. However, under the combined wind, current and wave loading, some vessel offsets are expected.

At a far vessel offset, the TDP will move away from the vessel while at a near offset, the TDP will move towards the vessel. For lazy wave riser, the same amount of vessel offset will cause less TDP movement than SCR due to the fact that the buoyancy arch section can compensate quite a lot of vessel motion.

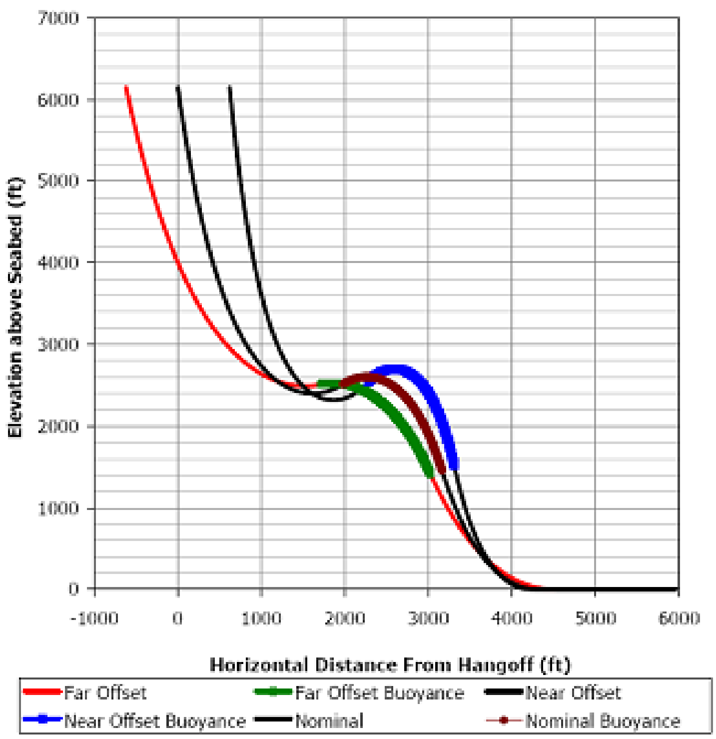


Fig. 4 Variation of lazy wave configuration with vessel offsets (Li and Nyuen 2010)

### 3.2 Bottom current

The TDP location is typically not sensitive to current loading directly acting on riser itself, especially if it is a near surface current. However, for bottom current, the impact on lower part of the catenary shape can be significant. In addition, monitoring the direction and magnitude of bottom current is much more difficult than surface current during riser installation. Ignoring the impact of bottom current can also lead to TDP mismatch. For a lazy wave riser which has the buoyancy section near bottom, the impact of bottom current can be significantly more pronounced than SCRs.

### 3.3 Seabed properties

#### 3.3.1 Seabed Slope/Profile

In riser analysis, for simplicity, a horizontal flat seabed is mostly assumed. However, in real world the seabed profile from survey data can be very complicated, and the seabed slope can be quite large. The configuration of lower part of catenary shape is controlled by the seabed slope/profile, so the TDP location is largely impacted by the seabed slope/profile. Although seabed survey is usually conducted before riser installation, the detailed profile at local riser touch down zone is typically not considered in current industry practice for installation analysis, and can thus lead to TDP location mismatch.

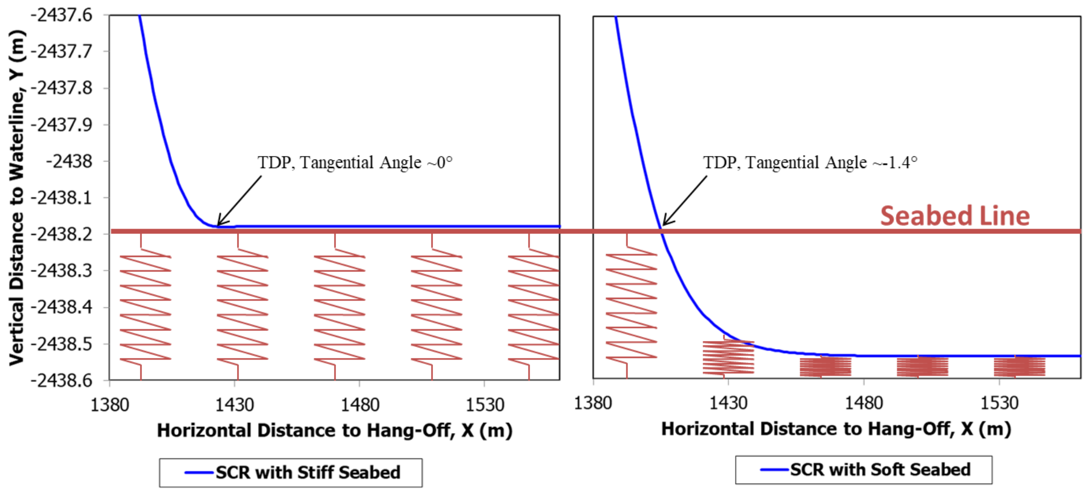


Fig. 5 Pipe-soil interact schematic

### *3.3.2 Seabed stiffness*

The seabed stiffness also impacts the TDP location, especially when the stiffness changes from very high stiffness to very low stiffness. The stiffness is essentially affecting the tangential slope of the TDP as shown in Fig. 5.

### *3.4 Riser wet weight and buoyancy uplift force*

Riser wet weight is not included in the SCR catenary Eqs. (1) and (2). Hence, it should not impact the TDP location. On the other hand, the wet weight and buoyancy uplift force are included in the LWSCR catenary Eq. (3). It is expected that TDP moves near to vessel when either increasing the riser wet weight or reducing the buoyancy uplift force.

## **4. Numerical validation and discussion**

To quantify the impact of each potential factor to the TDP location of catenary risers, numerical validation using FEA software, OrcaFlex, is conducted for a generalized project with SCR and LWSCR configuration options. The whole riser is modelled using beam element, and based on previous study by Hu *et al*. (2014) the global response of the riser can be accurately captured by this element type. For the case with vessel offsets, the suspended catenary lengths and corresponding projected horizontal lengths from theoretical equations are also provided.

### *4.1 Numerical example and base configurations*

A subsea riser attached to a semi-submersible platform is considered in this numerical study. A 10-in riser pipe is attached to a porch 125ft below waterline with 12° hang-off angle in an 8000 ft water depth. More details can be found in Table 1.

Table 1 Key parameters

| Parameters | Values |
|---|---|
| Hang-Off Angle | 12° |
| Hang-Off Depth | -38.1m (-125 ft) |
| Water Depth | 2438.4 m (8000 ft) |
| Pipe OD | 0.27305 m (10.75 in) |
| Straked Riser Mass | 315.7 kg/m |
| Straked Riser Wet Weight (Empty) | 151 kg/m (empty) |
| Straked Drag OD | 0.4493 m |
| Internal Fluid Density | 600 kg/m$^3$ |
| Buoyed Riser Mass | 882 kg/m |
| Buoyancy Drag OD | 1.2 m |
| Buoyed Riser Wet Weight | -277 kg/m (empty) |

Table 2 Base case parameter for catenary configurations

| Parameters | SCR | LWSCR |
|---|---|---|
| Hang-Off Tangent Angle, $\theta_1$ | -78° | -78° |
| Height, Y | 2400.3 m (7875 ft) | 2400.3 m (7875 ft) |
| Straked Riser Wet Weight (Filled with Operational Fluid), $m_1$ | 168 kg/m | 168 kg/m |
| Buoyed Riser Wet Weight (Filled with Operational Fluid) , $m_2$ | ~ | -261 kg/m |
| Upper Catenary Length, S1 | ~ | 2500 m |
| Buoyancy Section Length, S2 | ~ | 600 m |
| Seabed Slope | Flat | Flat |
| Seabed Stiffness | 400 kN/m/m | 400 kN/m/m |
| Vessel Offset | No | No |
| Bottom Current | No | No |
| FlexJoint Stiffness | See Fig. 6 | See Fig. 6 |

Table 3 Catenary configurations

| Parameters | From FEA | From Catenary Equations |
|---|---|---|
| Hang-Off Tangent Angle, $\theta_1$ | 78° | 78° |
| Height, $Y$ | 2400.3 m (7875 ft) | 2400.3 m (7875 ft) |
| **SCR**, Total Suspended Length, $S$ | 2963.49 m | 2964.12 m |
| **SCR**, Horizontal Projected Length, $X$ | 1419.56 m | 1419.36 m |
| **LWSCR**, Total Suspended Length, $S$ | 3819.0 m | 3816.9 m |
| **LWSCR**, Horizontal Projected Length, $X$ | 2382.52 m | 2380.28 m |

The base case parameters for catenary riser configurations are summarized in Table 2. It should be noted that the strake riser wet weight, flexjoint stiffness and seabed stiffness are not used in the SCR catenary equation, while the latter two items are not used in LWSCR catenary equations.

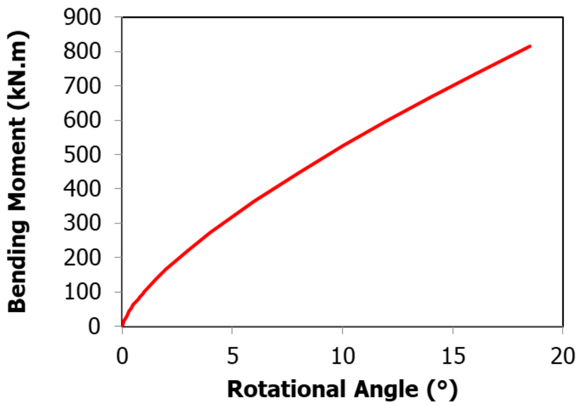


Fig. 6 FlexJoint rotational stiffness

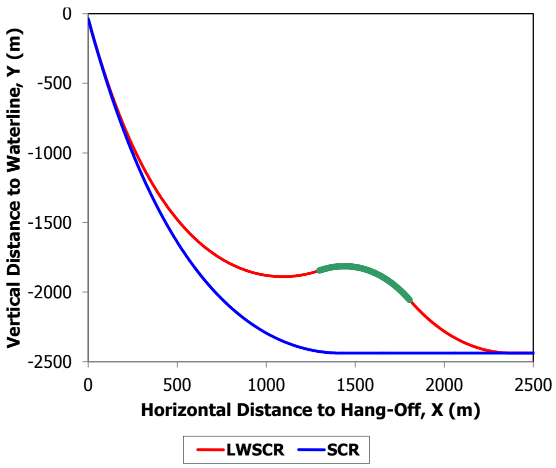


Fig. 7 Base configurations for SCR and LWSCR

The base configurations for SCR and LWSCR using the parameters in Table 2 are shown in Fig.7. The total suspended lengths ($S$) and projected horizontal lengths ($X$) from FEA and catenary equations are summarized in Table 3.

### *4.2 Vessel offsets*

In the riser installation stage, the offshore platform can offset in the environmental direction due to environmental loading. In this study, vessel offset in the near and far direction is considered from -5% (Far) to +5% (Near) of water depth. These large offsets are set to study the impact of vessel offsets on the TDP mismatch and should not be used as a reference to set the allowable offset for installation criteria. The results from both FEA and equations are summarized in the following table.

Based on the results in Table 4, the SCR TDP positions from both FEA and equation calculation move almost the same distance as vessel offset when vessel moves in near direction, while the SCR TDP moves almost 1.5 times the vessel offset when vessel moves in far direction. On the other hand, the TDP movement for LWSCR due to vessel offset is not as sensitive to the top vessel offset as SCR due to the decoupling effect from the buoyancy section.

### *4.3 Bottom current*

In-plane bottom current profile (see Fig. 8) is applied to the base configuration. The amplitude varies from -100% to +100% with 20% increment. The TDP coordinates results are summarized in Table 5, which indicate both riser systems are susceptible to bottom current. And their TDPs move in the opposite direction when facing the same current. For this specific bottom current profile, TDP of SCR configuration is more sensitive than LWSCR.

Table 4 TDP horizontal coordinates with various vessel offsets

| Vessel Offset | SCR, m | | | | LWSCR, m | | | |
|---|---|---|---|---|---|---|---|---|
| % of WD, 8000 ft | FEA | FEA Change | Equations | Equations Change | FEA | FEA Change | Equations | Equations Change |
| -5% (-121.92 m) | 1592.43 | 172.87 | 1592.46 | 173.10 | 2435.50 | 52.98 | 2434.08 | 53.80 |
| -4% (-97.54 m) | 1554.46 | 134.90 | 1554.91 | 135.55 | 2422.50 | 39.98 | 2421.54 | 41.26 |
| -3% (-73.15 m) | 1518.48 | 98.92 | 1518.9 | 99.54 | 2411.51 | 28.99 | 2409.90 | 29.62 |
| -2% (-48.77 m) | 1484.51 | 64.95 | 1484.35 | 64.99 | 2400.51 | 17.99 | 2399.24 | 18.96 |
| -1% (-24.38 m) | 1451.54 | 31.98 | 1451.19 | 31.83 | 2391.52 | 9 | 2389.40 | 9.12 |
| 0 | 1419.56 | 0 | 1419.36 | 0 | 2382.52 | 0 | 2380.28 | 0 |
| +1% (+24.38 m) | 1389.59 | -29.97 | 1388.81 | -30.55 | 2374.52 | -8 | 2371.82 | -8.46 |
| +2% (+48.77 m) | 1360.62 | -58.94 | 1359.46 | -59.90 | 2366.53 | -15.99 | 2363.96 | -16.32 |
| +3% (+73.15 m) | 1332.64 | -86.92 | 1331.28 | -88.08 | 2359.53 | -22.99 | 2356.65 | -23.63 |
| +4% (+97.54 m) | 1305.67 | -113.89 | 1304.22 | -115.14 | 2352.53 | -29.99 | 2349.83 | -30.45 |
| +5% (+121.92 m) | 1281.69 | -137.87 | 1278.22 | -141.14 | 2346.54 | -35.98 | 2343.49 | -36.79 |

Table 5 TDP horizontal coordinates with various bottom currents

| Bottom Current Speed, % | SCR, m | Change, m | LWSCR, m | Change, m |
|---|---|---|---|---|
| -100% | 1383.60 | -35.96 | 2394.53 | 12.01 |
| -80% | 1396.59 | -22.97 | 2389.53 | 7.01 |
| -60% | 1406.58 | -12.98 | 2386.52 | 4 |
| -40% | 1414.57 | -4.99 | 2384.52 | 2 |
| -20% | 1418.57 | -0.99 | 2382.52 | 0 |
| No Current | 1419.56 | 0.00 | 2382.52 | 0 |
| 20% | 1421.56 | 2.00 | 2381.52 | -1 |
| 40% | 1425.56 | 6.00 | 2380.52 | -2 |
| 60% | 1432.55 | 12.99 | 2378.52 | -4 |
| 80% | 1442.54 | 22.98 | 2376.51 | -6.01 |
| 100% | 1454.53 | 34.97 | 2373.51 | -9.01 |

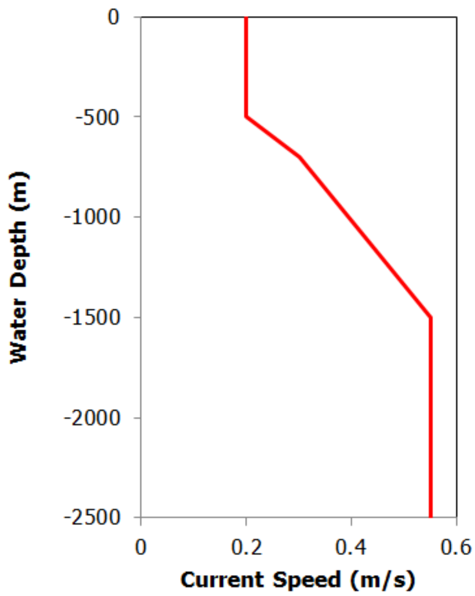


Fig. 8 Bottom current profile

## *4.4 Seabed properties*

### *4.4.1 Seabed slope*

Seabed slopes from -4° to +4° with 1° increment are considered in the analysis. The results are summarized in Table 6. The impact of seabed slope on the TDP locations are more severe in the SCR configuration comparing to the LWSCR configuration. This can be explained as the vertical length difference (SCR 7875 ft vs. LWSCR Lower 1241 ft) and hang-off tangential angle (SCR 78° vs. LWSCR Lower 55.6°) between SCR and the lower catenary of LWSCR. In another word, for deeper water depths and larger hang-off tangential angles, the impact of the seabed slope will be larger.

Table 6 TDP horizontal coordinates with various seabed slopes

| **Seabed Slope, °** | **SCR, m** | **Change, m** | **LWSCR, m** | **Change, m** |
|---|---|---|---|---|
| -4 | 1377.33 | -42.23 | 2385.22 | 2.70 |
| -3 | 1387.55 | -32.01 | 2383.48 | 0.96 |
| -2 | 1398.00 | -21.56 | 2382.95 | 0.43 |
| -1 | 1408.68 | -10.88 | 2382.63 | 0.11 |
| 0 | 1419.56 | 0 | 2382.52 | 0 |
| 1 | 1430.66 | 11.10 | 2382.62 | 0.10 |
| 2 | 1441.94 | 22.38 | 2382.94 | 0.42 |
| 3 | 1452.41 | 32.85 | 2384.47 | 1.95 |
| 4 | 1464.05 | 44.49 | 2386.21 | 3.69 |

Table 7 TDP horizontal coordinates with various seabed stiffnesses

| Seabed Stiffness, kN/m/m | SCR, m | Change, m | LWSCR, m | Change, m |
|---|---|---|---|---|
| 50 | 1415.57 | -3.99 | 2378.52 | -4 |
| 100 | 1417.57 | -1.99 | 2380.52 | -2 |
| 200 | 1418.57 | -0.99 | 2381.52 | -1 |
| 400 | 1419.56 | 0 | 2382.52 | 0 |
| 800 | 1420.56 | 1 | 2383.52 | 1 |
| 1300 | 1421.56 | 2 | 2383.52 | 1 |

Table 8 TDP horizontal coordinates with various vessel offsets

| Steel Mass | SCR, m | | LWSCR, m | | | |
|---|---|---|---|---|---|---|
| or Buoyed Section Mass | Steel Mass | Change | Steel Mass | Change | Buoy Mass | Change |
| -5% | 1420.57 | 1.01 | 2445.52 | 64 | 2486.50 | 104.98 |
| -4% | 1420.57 | 1.01 | 2431.52 | 50 | 2465.51 | 83.99 |
| -3% | 1420.57 | 1.01 | 2419.52 | 38 | 2445.52 | 64 |
| -2% | 1420.57 | 1.01 | 2405.52 | 24 | 2423.52 | 42 |
| -1% | 1419.57 | 0.01 | 2393.52 | 12 | 2403.52 | 22 |
| 0 | 1419.56 | 0 | 2381.52 | 0 | 2381.52 | 0 |
| 1% | 1419.56 | 0 | 2369.52 | -12 | 2361.52 | -20 |
| 2% | 1419.56 | 0 | 2359.52 | -22 | 2339.52 | -42 |
| 3% | 1419.56 | 0 | 2349.52 | -32 | 2319.52 | -62 |
| 4% | 1419.56 | 0 | 2339.52 | -42 | 2299.52 | -82 |
| 5% | 1419.56 | 0 | 2329.52 | -52 | 2279.52 | -102 |

#### *4.4.2 Seabed stiffness*

Seabed stiffnesses from 50 kN/m/m to 1300 kN/m/m are considered in this study. The results of the TDP coordinates are summarized in Table 7. The impact of seabed stiffness on TDP coordinates is slightly more severe for SCR configuration than LWSCR configuration though both are not that sensitive for analyzed cases. There is a trend that TDP locations are more sensitive when the soil stiffness is smaller.

### *4.5 Riser wet weight and buoyancy uplift force*

The changes of riser wet weight change and buoyancy uplift force are realized by changing the steel pipe in-air mass and buoyed section in-air mass by -5% to +5% with 1% increment. The results are summarized in Table 8. As predicted, there is almost no impact on SCR TDP location when varying the steel mass. On the other hand, LWSCR is very sensitive to both the riser wet weight and buoyancy uplift force change.

### *4.6 Discussion of TDP mismatch impact on riser performance*

The TDP displacement changes the riser configuration shapes, hence, it results in the variation of the riser tension and bending moment, which impacts the riser strength responses and fatigue performances. The temporary TDP displacements due to temporary offsets and bottom currents during installation are not expected to have any long term strength and fatigue impacts. On the other hand, the permanent platform offset or unaccounted seabed slope is expected to impact the riser performances. The maximum touchdown zone (TDZ) API RP 2RD stress responses with different vessel offsets for both SCR and LWSCR are summarized in Table 9.

For SCR, the observations are listed below:

- The maximum TDZ stress increases with offsets in any direction from the riser configuration with -1% WD offset.
- The static stress range between +1% WD offset and -1% WD offset from the corresponding vessel offset shows a similar trend: larger the corresponding offset, larger the static stress range.
- Though the SCR fatigue performance will be dependent on the dominant wave period, the fatigue performance trend is generally following the same trend as the static stress range does.

For the LWSCR configurations studied in this paper, the observations are listed below:

- The maximum TDZ stress increases with larger near direction offsets and decreases with larger far direction offset.
- The static stress range between +1% WD offset and -1% WD offset from the corresponding vessel offset shows a similar trend: larger the corresponding offset, larger the static stress range.
- It should be noted that the riser wave fatigue performances also depend on the initial LWSCR configuration and dominant wave period. The trend of the static stress range variation can only be treated as an indicator.

Table 9 Maximum TDZ API RP with various vessel offsets

| | **API RP 2RD Stress - TDZ (MPa)** | | | |
|---|---|---|---|---|
| **Offset/WD** | **SCR** | | **LWSCR** | |
| | **Maximum** | **Static Stress Range(1)** | **Maximum** | **Static Stress Range(1)** |
| -5% | 77.76 | - | 76.01 | - |
| -4% | 76.89 | -1.52 | 76.37 | 0.83 |
| -3% | 76.24 | -1.05 | 76.85 | 1.05 |
| -2% | 75.84 | -0.57 | 77.43 | 1.26 |
| -1% | 75.68 | -0.09 | 78.11 | 1.46 |
| 0 | 75.75 | 0.41 | 78.89 | 1.65 |
| +1% | 76.08 | 0.92 | 79.76 | 1.82 |
| +2% | 76.67 | 1.45 | 80.71 | 1.99 |
| +3% | 77.53 | 2.00 | 81.75 | 2.16 |
| +4% | 78.67 | 1.65 | 82.87 | 2.32 |
| +5% | 79.18 | - | 84.07 | - |

(1) Stress range is defined as the difference between +1% WD and -1% WD of current offset.

## 5. Conclusions

Theoretical equations have been discussed for both SCR and LWSCR configurations. Numerical validation has been conducted for the catenary riser configurations. Sensitivity studies for each critical factor towards the TDP location of catenary riser are conducted to quantify their impacts.

The key conclusions for SCR configuration are:

- The TDP moves along with vessel offset: 1.5 times in the far direction and almost the same length in the near direction.
- The impact of bottom current on TDP location is not a linear effect. The larger the current, the larger displacement the TDP will move.
- Seabed slope has large impact on SCR TDP locations; Seabed stiffness can also impact the TDP locations when large stiffness is used while the measured results are very small.
- Riser weight has negligible effect on SCR TDP locations.

The key conclusions for LWSCR configurations are:

- The TDP moves along with vessel offset but not as sensitive as the SCR configuration because the separation effect of buoyancy section: less than half of the vessel offset.
- For the analyzed in-plane bottom current profile and LWSCR configuration, the TDP location is not very sensitive. However, it can be more sensitive to variations of current profiles or current directions.
- Seabed slope and seabed stiffness has much smaller impact on LWSCR TDP location than that of SCR.
- The riser wet weight and buoyancy uplift force has very significant impact on LWSCR configuration and its TDP locations.

A few recommendations based on the analysis are listed below:

- If the key contributor to the TDP mismatch is vessel offset or current, no additional work is needed for checking long term fatigue response of the riser because vessel offsets and bottom currents normally occur as a short time event, and the TDP location will move back to the designed location in the long term; However if vessel offset or current during installation are severe enough to cause short term fatigue damage, fatigue damage during installation needs to be checked. And if the installation fatigue is found to be significant or exceeds the allowable budget set during the design, total combined fatigue damage needs to be re-calculated. In that case, load sequence effects can play an important role. Yin *et al.* (2014), Yin *et al.* (2010) studied the effect of load sequence effects in fatigue estimation in variable amplitude loading.
- In the global analysis for riser design, usually flat seabed is used. However, when creating the general arrangement (GA) drawings, modeling the seabed profile and correct seabed stiffness in the FEA are strongly recommended; If seabed stiffness for installation is not available, the value used in the GA drawing model should be added as notes in the drawing.
- If riser weight or buoyancy uplift force deviates from the design data after installation for LWSCR configuration, re-evaluation of the fatigue response with the as-built configuration

is strongly recommended since the lazy wave shape change can change the TDP fatigue performance per Section 4.6.

## References

Andrade, E.Q., Aguiar, L.L., Senra, S.F., Siqueira, E.F.N., Torres, A.L.F.L. and Mourelle, M.M. (2010), Optimization Procedure of Steel Lazy Wave Riser Configuration for Spread Moored FPSOs in Deepwater Offshore Brazil, OTC 20777.

Antony, A., Parambath, A., Yue, B., Man, K. and Thethi, R. (2017), Cost Savings Associated with Improved VIM Prediction Accuracy, OTC 27889.

Hoffman, J., Yun, H. and Modi, A. (2010), Parque das Conchas (BS-10) Pipeline, Flowline and Riser System Design, Installation and Challenges, OTC 20650.

Singh, R.R. and Bhatt, M. (2010), Engineering Mathematics, A Tutorial Approach, Tata McGraw Hill Education Private Limited.

Hu, G., Campbell, M. and Huang, C. (2014), Dynamic Plastic Deformation of Deepwater Steel Catenary Risers under Extreme Cyclic Compressive Loading. Oil and Gas Facilities.

Li, S. and Nyuen, C. (2010), Dynamic Response of Deepwater Lazy-Wave Catenary Riser. Deep Offshore Technology International, Amsterdam, Netherlands.

Orcina ltd. (2018), OrcaFlex 10.2a. https://www.orcina.com/Resources/index.php.

Queau, L.M., Kimiaei, M. and Randolph, M.F. (2013), Lazy Wave Catenary Risers: Scaling Factors and Analytical Approximation of The Static Stress Range in The Touchdown Zone. OMAE 10273.

Santala, M.J., Constantinides, Y., Koska, R., Krapf, C. and Walters, D.S. (2017), SCR Life Extension through Managed Shape Change, OTC 27597.

Thomas, B., Benirschke, A. and Sarkar, T. (2010), Parque das Conchas (BC-10) Steel Lazy Wave Riser Installation, Pre-abandonment, Recovery and Transfer Challenges, OTC 20605.

Wang, J., Duan, M., Fan, J. and Liu, Y. (2013), Static Equilibrium Configuration of Deepwater Steel Lazy-Wave Riser, ISOPE TPC157

Yue, B., Campbell, M., Walters, D., Thompson, H. and Raghavan, K. (2010), Improved SCR Design for Dynamic Vessel Applications, OMAE 20406.

Yue, B., Walters, D., Yu, W., Raghavan, K. and Thompson, H. (2011), Lazy Wave SCR on Turret Moored FPSO, ISOPE TPC871.

Yin, F., Cerkovnik M. and Conle A. (2014), Assessment of Fatigue Damage from Variable Amplitude Loads in Risers, ISOPE TPC0128.

Yin, F., Fatemi, A. and Bonnen, J. (2010), "Variable amplitude fatigue behavior and life predictions of case-hardened steels", *Int. J. Fatigue*, **32**, 1126-1135.

*MK*